

Highest Ionic Conductivity of BIMEVOX (ME = 10% Cu, 10% Ga, 20% Ta): Computational Modeling and Simulation

Akram La Kilo^{1*}, Alberto Costanzo², Daniele Mazza², Muhamad Abdulkadir Martoprawiro³, Bambang Prijamboedi³, and Ismunandar³

¹Department of Chemistry, Universitas Negeri Gorontalo, Jl. Jenderal Soedirman No. 6 Gorontalo 96128, Indonesia

²Dipartimento di Scienza dei Materiali e Ingegneria Chimica, Politecnico di Torino, Corso Duca degli Abruzzi 24, 10129 Torino, Italy

³Inorganic and Physical Chemistry Research Group, Faculty of Mathematics and Natural Sciences, Institut Teknologi Bandung, Jl. Ganesha No. 10, Bandung 40132, Indonesia

* Corresponding author:

email: akram@ung.ac.id

Received: January 1, 2019

Accepted: June 25, 2019

DOI: 10.22146/ijc.42635

Abstract: BIMEVOX had the potential to play an important role in solid oxide fuel cell, especially as the electrolyte due to their high ionic conductivity. In this work, oxide ion migrations of γ -Bi₂VO_{5.5} and BIMEVOX were simulated using density functional theory (DFT), Mott-Littleton method, and molecular dynamics simulation. In γ -Bi₂VO_{5.5}, there were oxygen vacancies at the equatorial position in the vanadate layers. These vacancies could facilitate oxide ions migration. The Enthalpy of the oxide migration for γ -Bi₂VO_{5.5} based on DFT calculation was 0.38 eV, which was in good agreement with experimental results. The γ -Bi₂VO_{5.5} can be stabilized by partial substitution of V⁵⁺ with Cu²⁺, Ga³⁺, and Ta⁵⁺. Defect simulation results using the Mott-Littleton method showed that the total maximum energies of region II were achieved at concentrations of 10, 10, and 20%, respectively, for Cu²⁺, Ga³⁺, and Ta⁵⁺. The calculated concentration of Cu²⁺, Ga³⁺, and Ta⁵⁺ was in good agreement with those of experiment results, where the highest ionic conductivity was obtained. The results of the molecular dynamics simulation showed that the activation energies of oxide ion migration in γ -Bi₂VO_{5.5} and BIMEVOX (ME = Cu and Ta) were 0.19, 0.21, and 0.10 eV, respectively, close to experimental values.

Keywords: simulation; vacancy defect; γ -Bi₂VO_{5.5} and BIMEVOX; ionic migration

■ INTRODUCTION

Solid electrolyte materials with high oxide ion conductivity intensively investigated in order to have a solid oxide fuel cell (SOFC). One of the oxide materials that had high oxide ion conductivity and the potential application was Bi₂V_{1-x}Me_xO_{5.5-σ} (BIMEVOX), where ME was dopant [1-3]. Dopant at a certain concentration plays an important role in improving the ease of oxygen ions migration of Bi₂VO_{5.5} [4-5]. Therefore, in addition to the migration path of oxygen ions, the search for a type of dopant with a certain concentration was needed to obtain BIMEVOX with high conductivity. The computational simulation method could be conducted first to predict the ease of ion migration.

BIMEVOX was a family of oxides derived from Bi₂VO_{5.5} and obtained by doping into the vanadium site of Bi₂VO_{5.5} by aliovalent or isovalent metal cations (ME). The structure of Bi₂VO_{5.5} could be derived from Bi₂MoO₆ and δ -Bi₂MoO₆ by the formation of oxygen vacancies in the metal oxygen layers; thus, the compound can be formulated as (Bi₂O₂)(VO_{3.5}π_{0.5}), where π was corresponding to the intrinsic oxygen vacancies [6-7].

The Bi₂VO_{5.5} goes to several structural transformations and known had several polymorphs, but essentially there were only three main polymorphs, namely α, β, and γ -Bi₂VO_{5.5} with the transformations: α → β at 720 K and β → γ at 840 K. The structures of α and

β -phases were more ordered, larger in unit cell and had lower conductivity. At the high temperature, γ -phase was formed and had a conductivity of 0.2 Scm^{-1} at 943 K [6]. The $\gamma\text{-Bi}_2\text{VO}_{5.5}$ can be stabilized by partial substitution of V^{5+} with other metal cations (ME) [8-9]. The substitution does not only stabilize the structure but also increases ionic conductivity due to the creation of vacancies [10-11]. Therefore, the computational simulation carried out in this study was the gamma phase of $\text{Bi}_2\text{VO}_{5.5}$ and BIMEVOX (ME = Cu^{2+} , Ga^{3+} , and Ta^{5+}).

The experimental results of BIMEVOX compounds showed the contribution of electrons that affected BIMEVOX conductivity [12]. Moreover, the texture of compounds, surface conditions, pore existence, and the presence of impurities affect ionic conductivity. A single phase of BITAVOX could not be obtained by synthesis [13]. Dereeper et al. reported that BITAVOX conductivity increases with the increase in Ta dopant concentration. BIGAVOX had a smaller conductivity due to the contribution of electron conductivity [13]. Therefore, the single phase of the gamma- $\text{Bi}_2\text{VO}_{5.5}$ and BIMEVOX (Cu^{2+} , Ga^{3+} , and Ta^{5+}) through computational modeling and simulation was important to be conducted to predict the possibility of ease of migration of oxygen ions without the presence of electron conductivity.

Experimental studies on the oxide ionic conductivity of BIMEVOX have been reported elsewhere [14]. However, the experimental study could not reveal the detail of the mechanism of oxide ion conductivity and the role of dopant in the BIMEVOX on the structural properties. Computational studies could be used to study many material properties efficiently in order to save time and cost as well as to provide more detail mechanisms at the atomic level. Some computation study on the layered structure of Aurivillius phases similar to BIMEVOX has been carried out and reported [15-16]. It could reveal defect energies and maximum dopant concentrations in Aurivillius as ferroelectric material. From our best knowledge, the computational study on BIMEVOX was not reported yet.

Here, we report the computational study on BIMEVOX and its parent structure that cover the trajectory of ionic oxide in $\gamma\text{-Bi}_2\text{VO}_{5.5}$ and defect energy

of BIMEVOX. The study was aimed to investigate the oxide ion pathways that were possible in the V^{5+} coordination environments of $\gamma\text{-Bi}_2\text{VO}_{5.5}$ as well as to predict dopant concentrations of Cu^{2+} , Ga^{3+} , and Ta^{5+} that give the higher ionic conductivity. Subsequently, transport properties and activation energy of migration of oxygen ions of the parent compound and BIMEVOX (ME = Cu^{2+} and Ta^{5+}), which were predicted to have the highest ionic conductivity, were simulated using the molecular dynamics method. Those dopants were selected because of their ionic radius close to the ionic radius of V^{5+} . This means that the dopant with an ionic radius close to the V^{5+} radius could enhance the conductivity [17].

■ COMPUTATIONAL METHODS

Enthalpy of Oxide Ion Migration

The enthalpies of oxide ion migration of $\gamma\text{-Bi}_2\text{VO}_{5.5}$ were calculated by using a computational simulation method that is based on density functional theory (DFT). This simulation used the CASTEP code of Material Studio Modeling from Accerys, series number 3.2.00, in Politecnico di Torino [18]. The methodology for electronic structure calculations in CASTEP is as follows: set of one-electron Schrodinger (Kohn-Sham) equations are solved using the plane-wave pseudopotential approach. The wave functions are expanded in a plane wave basis set defined by the use of periodic boundary condition and Bloch's Theorem. The electron-ion potential is described by means of *ab initio* pseudopotentials within both norm-conserving and ultrasoft formulations. Direct energy minimization schemes are used to obtain self-consistently, the electronic wave functions and its corresponding charge density. Lattice optimization is initially performed using exchange-correlation energy functions of Perdew-Burke-Ernzerhof (GGA-PBE). Structural optimizations were implemented to determine the best functional approximation to perform in examining the enthalpy of $\gamma\text{-Bi}_2\text{VO}_{5.5}$ at various oxygen positions of the tetragonal vanadate layer. A k-point grid of $1 \times 1 \times 1$ generated using the Monkhorst-Pack method for Brillouin zone sampling with an energy cut-off of 600 eV.

Atomistic simulation and Molecular Dynamic

The main samples used in this simulation were of two types, namely (i) the tetragonal structure of γ - $\text{Bi}_2\text{VO}_{5.5}$ with an I4/mmm space group as reported by Mairesse et al. [17] and (ii) the tetragonal structure of γ - $\text{Bi}_2\text{VO}_{5.5}$ with P1 space group modified from the first structure. The two structures were then doped with a dopant (ME) of Cu, Ga, and Ta to obtain BIMEVOX compounds. In the first structure, the simulation method applied is atomistic simulation using GULP [19]. The simulation aims to calculate defect energy while predicting the ease of migration of oxygen ion in BIMEVOX based on the increase in dopant concentration. Meanwhile, the second structure applied molecular dynamics to determine the property of transport or activation energy of the migration of oxygen ions using the DLPOLY code [20]. Both simulation methods use Buckingham's short range potential defined:

$$\theta_{ij} = A_{ij} \exp\left(-\frac{r_{ij}}{\rho_{ij}}\right) - \frac{C_{ij}}{r_{ij}^6} \quad (1)$$

where A_{ij} , ρ_{ij} and C_{ij} were constant parameters, and r_{ij} was the distance between i and j ions. The first term in Eq. (1) describes short-range repulsion, while the second term shows induced dipole (van der Waals interaction).

Using DL_POLY, different defect concentrations were simulated by creating a supercell of $4 \times 4 \times 4$ containing dopant concentrations (10% Cu and 20% Ta) and the respective amount of oxygen vacancies. The simulations were carried out for a step time of 0.0002 ps with an ensemble of constant temperature and volume (NVT) and algorithm of leapfrog that applied to the simulation box of 1088 ions.

Defect Energy of BIMEVOX

Calculation of energy defects in atomistic simulations is performed on the average structure of γ - $\text{Bi}_2\text{VO}_{5.5}$ and BIMEVOX with space group I4/mmm. The energy defect of BIMEVOX was calculated based on the Mott-Littleton method, which divides the crystal lattice into the two regions, namely regions I (inner sphere) and II (outer sphere). Region I is the spherical region surrounding defect, which is clearly in relaxation. Meanwhile, the region II is the outer spherical defect that

has relatively weak force, which is interpreted with the quasi-continuum approximation method. In this way, the lattice relaxation can be modelled effectively, and also the crystal is not as a simple rigid lattice where the diffusion of ions occurs. If the force on the region II is small, it can be assumed that the response of ions in this region is pure harmonic. There are two kinds of defects, namely impurity, and vacancy defects. Impurity defect with a defect center of V^{5+} is substituted partially with dopants of Cu^{2+} , Ga^{3+} , and Ta^{5+} , while the defect of oxygen vacancies are intrinsic defect as well as its being created in equatorial position of oxygen, O(3). The concentration of dopants, which substitutes V partially, was compensated by a reduction of concentrations of oxygen, O(3), to neutralize the charge in BIMEVOX structure. Defect energy calculations were performed at concentrations of 5, 10, 15, and 20% for each dopant, except for Ta^{5+} that was also carried out at the concentration of 25 and 30%.

RESULTS AND DISCUSSION

Geometry optimization of the parent structure, γ - $\text{Bi}_2\text{VO}_{5.5}$, was an initial procedure to check the structure stability. The structure of γ - $\text{Bi}_2\text{VO}_{5.5}$ reported by Mairesse et al. [17], tetragonal, space group I4/mmm, cell unit dimension, $a = 3.99176(4)$, $b = 3.99176(4)$, and $c = 15.4309(3)$ Å was used as a starting model. The mean V–O octahedron was engaged between eight Bi sites. However, due to the O(2) and O(3) split-sites, it was observed that there were several short O–O contacts; these preclude simultaneous occupation of many of these O sites, as shown in Fig. 1.

In fact, the V–O environment, which appears as an octahedron squashed along the c stacking direction, must be viewed as the result of a superimposed polyhedral. Indeed, by selecting appropriate O sites among those drawn, the classical O environments of the V cation are easily recognized as octahedron, tetrahedron, trigonal bipyramid, and tetragonal pyramid with interatomic distances compatible with O atomic size [10]. Therefore, the structure, that has high symmetry and contains oxygen vacancy, can be represented using by space group P1 that had no symmetry, as shown in Fig. 2.

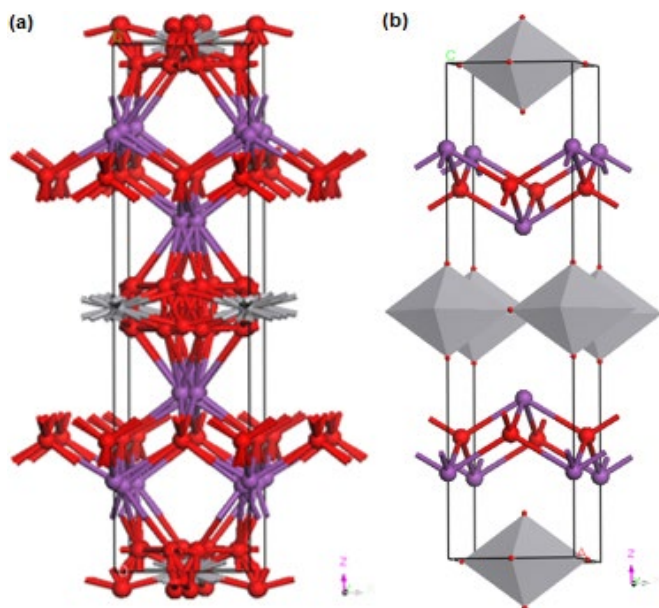


Fig 1. The crystal structures of $\text{Bi}_2\text{VO}_{5.5}$, (a) average crystallography structure, and (b) the refined structure oxygen vacancies were shown as oxygen atoms

The structure in Fig. 2 was one of the models of structure $\gamma\text{-Bi}_2\text{VO}_{5.5}$, showing a special vanadium-oxygen anions coordination environment. The structure that is simulated based on DFT indicates that the coordination environment of V cations by O(3) and oxygen vacancy are in good agreement with the crystallography site of $\gamma\text{-Bi}_2\text{VO}_{5.5}$ structure, as depicted in Fig. 1(a) and 2. Therefore, the crystal structure (Fig. 2) can be used as a starting structure to determine activation energy that represents oxygen jump and the easiness of ionic conduction.

Pathway of Oxide Ion Migration of $\text{Bi}_2\text{VO}_{5.5}$

Oxygen ions, which surround the vanadium ions (Fig. 3), could be divided into two types, namely apical site, O(2), and equatorial site, O(3). Geometry optimization results of a $\gamma\text{-Bi}_2\text{VO}_{5.5}$ show that the angle that occupied O(3)-V-vacant O(3) against V was 70 degrees, with O(3)-V bond length of 1.72 Å. Throughout this 70 degrees angle, all the different positions of O(3) are optimized to describe oxygen pathways in the equatorial site as shown in Fig. 3.

Based on the result of the optimized geometry of $\gamma\text{-Bi}_2\text{VO}_{5.5}$, the enthalpies of O(3) migration were calculated. The O(3) was moved from one position to the other vacant

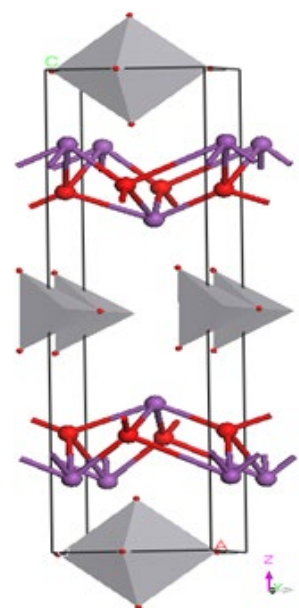


Fig 2. The one possibility of a structure that has V - O tetrahedral environment with oxygen vacancy in the equatorial site

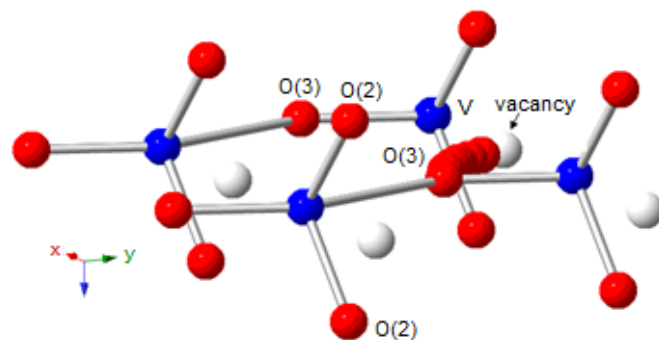


Fig 3. V coordination environments by oxide ions, O(3) equatorial oxygens and O(2) apical oxygens

position. The oxygen position with the highest energy, is in the middle between occupied position (initial position) and vacant position, as shown in Fig. 4.

The calculated activation energy of oxygen pathway was 0.38 eV and is in good agreement with experiment results, as given in Table 1.

Defect Energy of BIMEVOX

The calculation of defect energy was an important step to treat the lattice relaxation of point defect or migrating ion. In this study, the defect energy of BIMEVOX was calculated based on Mott-Littleton method. The number of ions involved in this defect energy

Table 1. Activation energies (eV) of oxygen ion motion in γ -Bi₂VO_{5.5} based on this simulation work and these obtained from experiment work

| Calculation (this work) | Experiment [ref.] | Description |
|-------------------------|-------------------|--|
| 0.384 | 0.3427 [14] | The temperature of 773 K, the sample obtained from a solid state reaction at sintering temperature of 1073 K for 10 and 12 h |
| | 0.35 [15] | The temperature of 873 K, the sample obtained from a solid state reaction at a sintering temperature of 1113 K for 5 h |
| | 0.4 [21] | High temperature, the sample obtained from solid state reaction at sintering temperature of 1103 k for 24 h |

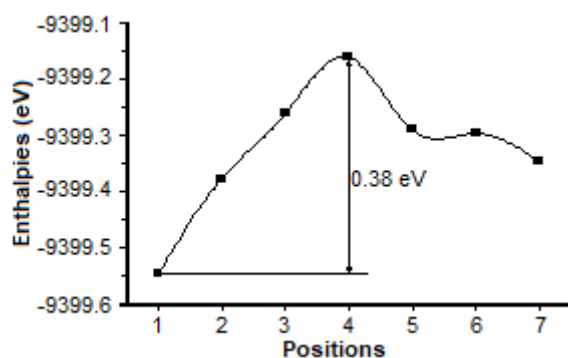


Fig 4. Enthalpies of oxygen migration as a function of the vacancy position in the γ -Bi₂VO_{5.5} structure

calculations was 5,604 ions for the region I and 103,016 ions for region II, with each radius was and 37 Å, respectively. The defect energy calculation results were summarized in Fig. 5.

The results of the defect energy calculations show that the defect energy values of region II vary according to the dopant type and concentration. Energy defect increases up to concentration of 10% for all dopants. However, for Ta⁵⁺, defect energy increases with the concentration of up to 20%. This was as expected because of Ta is isovalence to V, with valence = +5. Maximum defect energy values were reached at concentrations of 10% for Cu and Ga, and 20% for Ta, with values of -0.63, -1.57 and 8.98 eV, respectively. BICUVOX and BIGAVOX defect energies are more negative at a concentration of more than 10%, and the BITAVOX defect energies have the highest negative values at concentrations of 5 and 30% Ta. The negative values of defect energy show that the response of ion is pure harmonic and unstable. However, the BIMEVOXes can be synthesized at the concentrations.

Oxygen vacancies can be varied in accordance with

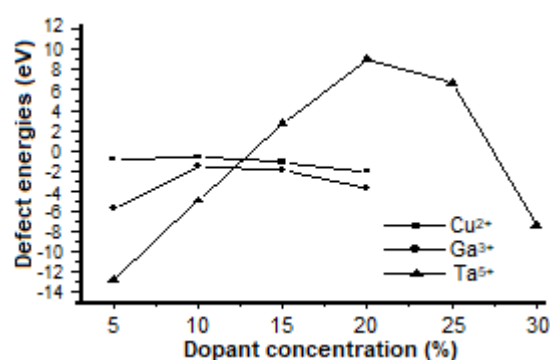


Fig 5. Energy defect in region II as a function of dopant concentration. BIMEVOX structure was expected to more conductive at a dopant concentration of 10% Cu, 15% Ga, and 20% Ta

the dopant valence and concentration. The dopant concentration increases the amount of oxygen vacancies in positions O(3). The preference of dopants affects symmetry and connectivity of polyhedral in the perovskite-like layer. Consequently, the performance of ionic conductivity is also expected to significantly depend on the defect structure and the effect of trapping on the diffusion pathway of oxygen [14]. Therefore, a stable structure is achieved when each dopant is at a certain concentration. Based on the defect energy values in this work, the concentration of dopants that stabilized γ -Bi₂VO_{5.5} and were predicted to have the highest conductivity are 10% for Cu, 10% for Ga, and 20% for Ta. At these concentrations, the cation polarizability of dopants is predicted to have achieved maximum value so that it facilitates the oxide ion diffusion process in the like-perovskite layers. Again, we predict that sequences of decreasing conductivity of BICUVOX, BIGAVOX, and BITAVOX are 10>15>20% for Cu; 10>15>20% for

Ga; and 20>25>15>30% for Ta, respectively, as Fig. 5. These are in agreement with the experimental results reported by Kant et al., Lazure et al., and Murasheva et al. [22-24]. At concentrations of more than 10% Cu, the ionic conductivity of BICUVOX decreases with the increasing vacancy because in its like-perovskite volume increase.

Concentration value of 10% Cu in this study is in good agreement with experimental results reported by Kant et al. [22] which showed the stable structure of BICUVOX at 10%, which has a grain pattern and uniform in size with adequate porosity, compared to the concentrations of 15 and 20%. Concentration of 20% Ta also in good agreement with the experimental results reported by Lazure et al., which states that the best conductivity for BITAVOX achieved at a concentration of 20% Ta [23]. BIGAVOX has also the highest conductivity at a concentration of 10% Ga for the gamma phase. According

to Kant et al., BIGAVOX has the highest conductivity at 10% for a beta phase, not the gamma phase [12]. While according to Murasheva et al. BIGAVOX phase was gamma at 10% Ga with more uniform grain [24].

Property of Transport and Activation Energy of BIMEVOX

Molecular dynamics simulations of $\text{Bi}_2\text{VO}_{5.5}$ starting with geometry optimization of the supercell ($4 \times 4 \times 4$) of $\text{Bi}_2\text{VO}_{5.5}$ using DLPOLY. In the perovskite layers of the supercell $\text{Bi}_2\text{VO}_{5.5}$, coordinations of V–O were 4 and 6 that arranged alternately between the bismuth layers (Fig. 6(a)). Coordination 4 of V–O (Fig. 6(c)) is square planar, and the coordination 6 is regular octahedral (Fig. 6). Since the superstructure is optimized, the ions were distorted in layers of bismuth and perovskite layer as shown in Fig. 6(d). The square planar of V–O turn

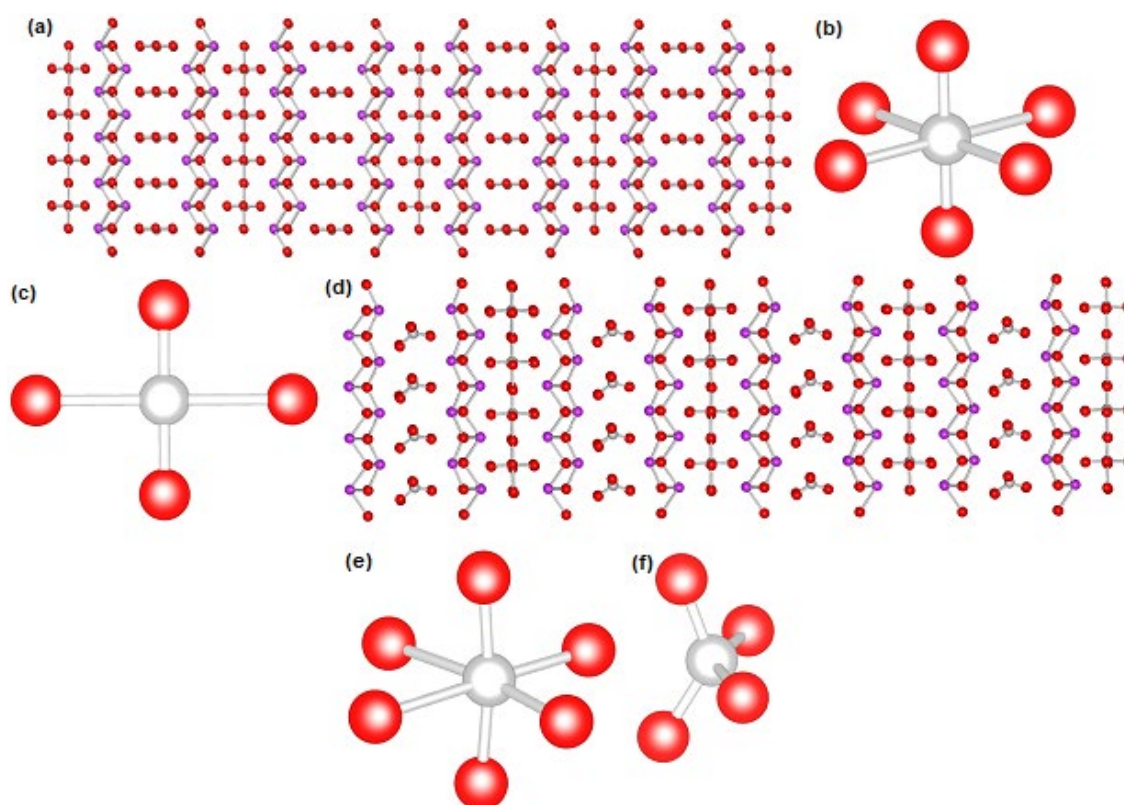


Fig 6. Super cell structure ($4 \times 4 \times 4$) $\text{Bi}_2\text{VO}_{5.5}$: (a) before optimization and (d) after optimization using DLPOLY code. In the perovskite-like layer, flat rectangular coordination (c) of the V–O has been changed into tetrahedral coordination (f), and the regular octahedral coordination (b) experienced distorted octahedral coordination (e). In an optimized structure, the ions in the bismuth layer are also distorted

into tetrahedral coordination (Fig. 6(f)), and the octahedral coordination is distorted (Fig. 6(e)). Therefore, the results of the supercell optimization of $\text{Bi}_2\text{VO}_{5.5}$ in accordance with the expected structure, which is also very similar to the results of the optimization of the unit cell $\text{Bi}_2\text{VO}_{5.5}$ using the DFT method.

The successful optimization of the $\text{Bi}_2\text{VO}_{5.5}$ supercell using DLPOLY has proven that this works well, and the short range potential of Buckingham between ions was also correct. Therefore, DLPOLY can be used to perform geometry optimization and molecular dynamics simulations of $\text{Bi}_2\text{VO}_{5.5}$. Furthermore, the transport properties (through molecular dynamics simulations) of $\text{Bi}_2\text{VO}_{5.5}$ studied by creating a supercell structure with VO coordinations were coordination mixtures of tetrahedral, coordination five, and octahedral. The coordination mixtures were representative to show the transport properties of the $\text{Bi}_2\text{VO}_{5.5}$ compound.

Molecular dynamics (MD) simulation were carried out on $\gamma\text{-Bi}_2\text{VO}_{5.5}$ and BIMEVOX that were predicted the easiest migration of oxygen ions as atomistic simulation results above, namely $\text{Bi}_2\text{Cu}_{0.1}\text{V}_{0.9}\text{O}_{5.35}$, $\text{Bi}_2\text{Ga}_{0.1}\text{V}_{0.9}\text{O}_{5.4}$, and $\text{Bi}_2\text{Ta}_{0.2}\text{V}_{0.8}\text{O}_{5.5}$. Before the MD simulation, the supercells of $\gamma\text{-Bi}_2\text{VO}_{5.5}$ and BIMEVOX were optimized first. The optimized structure was controlled at several temperatures to determine the properties of ion transport, such as mean square displacement (MSD) and activation energy. MSD was defined by the formula:

$$\text{MSD}_\beta(t) = \frac{1}{N} \sum_{i=1}^N [r_i(t) - r_i(0)]^2 \quad (2)$$

where $r_i(t)$ was the position of ion i at time t . In a perfect lattice, the MSD of component ions usually ranges from the average value. Meanwhile, in the defect lattice, there were mobile ions, such as O^{2-} in $\gamma\text{-Bi}_2\text{VO}_{5.5}$, where MSD increases over time. Fig. 7 shows the MSD data of the $\gamma\text{-Bi}_2\text{VO}_{5.5}$ plotted as a function of time at temperatures of 500, 700 and 1100 K. This shown that there were migrating oxide ions, where the temperature rise was followed by an increase in the diffusion of oxide ion.

From the plot of slope MSD can be determined by the diffusion coefficient (D_β) using correlation:

$$\text{MSD}_\beta(t) = 6D_\beta(t) - \text{MSD}_\beta(0) \quad (3)$$

where $\text{MSD}_\beta(0)$ was an atomic vibration factor arising from ion vibrations. The calculation of the diffusion coefficient at the three temperatures specified in Fig. 8. The calculation can be evaluated for the activation of ion migration using the Arrhenius relationship.

Based on the Arrhenius plot ($\ln D$ vs. $1/T$) above, the activation energy obtained is 0.19 eV. This value was a value commonly found in experiments, as reported by Joubert et al. [25].

MSD of $\text{Bi}_2\text{Cu}_{0.1}\text{V}_{0.9}\text{O}_{5.35}$ increases with increasing temperature as shown in Fig. 9. This indicated that the diffusion of oxide ions increases with increasing temperature. At a temperature of 500, 773 and 823 K, the MSD plot rises to a straight line compared to the MSD plot

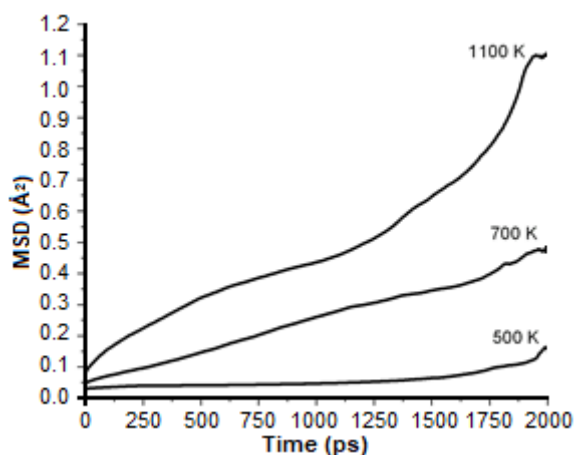


Fig 7. MSD of the oxide ions of $\gamma\text{-Bi}_2\text{VO}_{5.5}$ at temperatures of 500, 700, and 1100 K. The MSD receives an increase in temperature, which indicates that the diffusion of oxide ions also increases

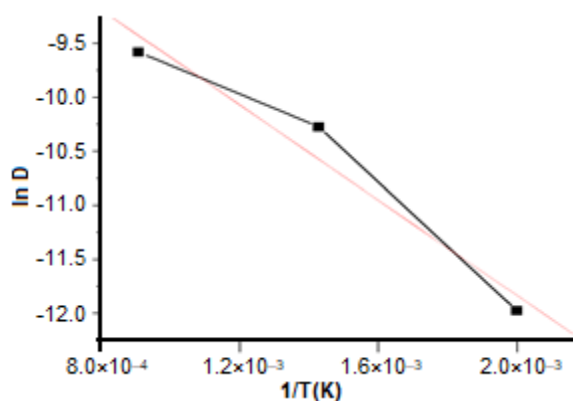


Fig 8. Plot $\ln D$ vs. $1/T$ for oxide ions of $\gamma\text{-Bi}_2\text{VO}_{5.5}$

at 873 K. At 873 K, the oxide ion migration rises rapidly to the timestep 160 ps, then the migration rises slowly to 480 ps, as shown in MSD with lines that are not straight (curved). At the timestep 160–480 ps, the migration of oxide ions was estimated to pass through the obstruction area. This kind of thing is observed in the migration of sodium ions of zeolites [26].

The diffusion coefficient of $\text{Bi}_2\text{Cu}_{0.1}\text{V}_{0.9}\text{O}_{5.35}$ at some temperatures was shown in Fig. 9. Based on this graph, the ion activation energy of $\text{Bi}_2\text{Cu}_{0.1}\text{V}_{0.9}\text{O}_{5.35}$ was 0.21 eV. This energy value was in accordance with the results of experiments reported by Guillodo et al. [27], but different from those reported by Krok et al. [28] and Simner et al. [29] as shown in Table 2. This difference can be caused by different synthesis methods.

The oxide ion MSD of $\text{Bi}_2\text{Ta}_{0.2}\text{V}_{0.8}\text{O}_{5.5}$ also increases with temperature rise (Fig. 10). Based on the plot of $\ln D$ (oxide ion diffusion coefficient) on $1/T$ (Fig. 10), the activation energy of the calculation result is 0.10 eV. Ion oxide MSD of $\text{Bi}_2\text{Ta}_{0.2}\text{V}_{0.8}\text{O}_{5.5}$ also increased with an increase in temperature. Based on the plot of \ln (oxide ion

diffusion coefficient) versus $1/T$, the activation energy was 0.10 eV.

This activation energy was smaller than the activation energy calculated from $\gamma\text{-Bi}_2\text{VO}_{5.5}$ and $\text{Bi}_2\text{Cu}_{0.1}\text{V}_{0.9}\text{O}_{5.35}$. This indicated that the conductivity of the $\text{Bi}_2\text{Ta}_{0.2}\text{V}_{0.8}\text{O}_{5.5}$ was greater than the conductivity of the two types of compounds.

The addition of dopant partially to the parent compound ($\gamma\text{-Bi}_2\text{VO}_{5.5}$) gives rise to environmental irregularities in the vanadate layer, which can inhibit oxygen migration. The irregularity is caused by different size of vanadium ($\text{V}^{5+} = 0.54 \text{ \AA}$) with dopants ($\text{Cu}^{2+} = 0.73 \text{ \AA}$; $\text{Ga}^{3+} = 0.62 \text{ \AA}$; $\text{Ta}^{5+} = 0.64 \text{ \AA}$) and increase of oxygen vacancy due to substitution of V^{5+} partially by Cu^{2+}

Table 2. The activation energy of $\text{Bi}_2\text{Cu}_{0.1}\text{V}_{0.9}\text{O}_{5.35}$ based on the experimental results

| Activation Energies (eV) | References |
|--------------------------|----------------------|
| 0.48 | Krok et al. [28] |
| 0.52 | Simner et al. [29] |
| 0.20 | Guillodo et al. [27] |

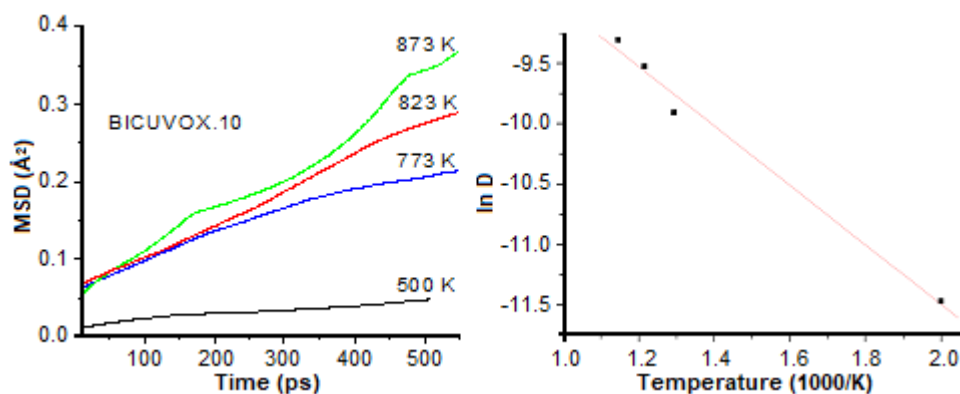


Fig 9. MSD and Plot of $\ln D$ vs. $1/T$ of oxide ion of $\text{Bi}_2\text{Cu}_{0.1}\text{V}_{0.9}\text{O}_{5.35}$

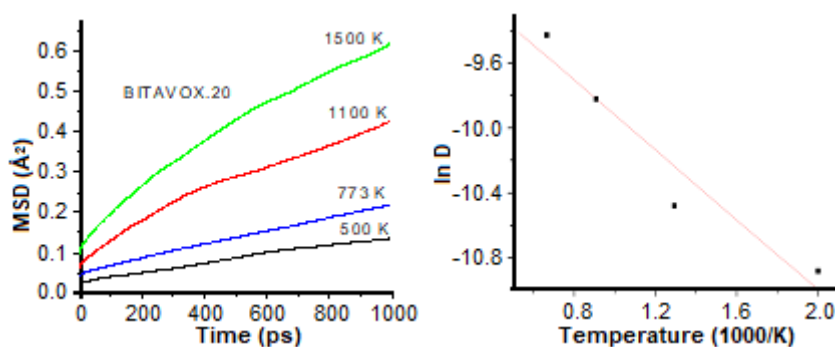


Fig 10. Oxide ion MSD and $\ln D$ vs. $1/T$ plot of $\text{Bi}_2\text{Ta}_{0.2}\text{V}_{0.8}\text{O}_{5.5}$

and Ga^{3+} . On the contrary, doping with Ta^{5+} does not add a vacancy because of Ta is isovalent with V.

The vacancy can cause a strong attraction between vacancies and V/dopants, thus increasing the activation energy of the migration of oxygen ion. The non-spherical d orbitals of Cu, with the configuration $3d^9$, also cause the vanadium environment to be distorted and can act as a trapping center in the process of oxygen ion migration.

Polarization of cations to oxygen ions can facilitate the hopping of oxygen ion to the vacancy site. This happens because the electron cloud of the oxide ion was pulled by the cation so that the oxide ion was easily moved from the site of the lattice. The polarization of the cations to the oxide ions that are getting stronger will further facilitate the oxide ions to migrate in the crystal lattice. Ta^{5+} cations, theoretically, will be stronger at polarizing oxide ions compared to Ga^{3+} and Cu^{2+} cations, because Ta^{5+} has a greater charge density. As a result, qualitatively it can be predicted that at the same concentration, the increase of ionic conductivity is $\text{BICUVOX} < \text{BIGAVOX} < \text{BITAVOX}$.

■ CONCLUSION

Computational simulation of ionic conductivity of BIMEVOX and $\gamma\text{-Bi}_2\text{VO}_{5.5}$ performed using DFT, Mott-Littleton method, and molecular dynamics simulation. The obtained enthalpy for $\gamma\text{-Bi}_2\text{VO}_{5.5}$ close to experimental results. Defect simulation using the Mott-Littleton method showed 10% Cu^{2+} , 10% Ga^{3+} , and 20% Ta^{5+} where the highest ionic conductivity was in good agreement with the experiment results. The results of the molecular dynamics simulation showed that the activation energies of oxide ion migration in $\gamma\text{-Bi}_2\text{VO}_{5.5}$ and BIMEVOX (ME = Cu and Ta close to experimental values. The addition of oxygen vacancy at $\gamma\text{-Bi}_2\text{VO}_{5.5}$ due to doping with aliovalent dopants, such as Cu and Ga, causes disordering polyhedral in the vanadate layer where oxygen ion migration takes place. In contrast, ordering polyhedral due to the inclusion of isovalent dopants such as Ta causes easier ion migration. To synthesize BIMEVOX compounds that are expected to have high ion conductivity, the concentrations of aliovalent and aliovalent dopants are 10% and 20%, respectively.

■ REFERENCES

- [1] Cho, H.S., Sakai, G., Shimanoe, K., and Yamazoe, N., 2005, Preparation of BiMeVO_x (Me= Cu, Ti, Zr, Nb, Ta) compounds as solid electrolyte and behavior of their oxygen concentration cells, *Sens. Actuators, B*, 109 (2), 307–314.
- [2] Chmielowiec, J., Paściak, G., and Bujło, P., 2008, Ionic conductivity and thermodynamic stability of La-doped BIMEVOX, *J. Alloys Compd.*, 451 (1-2), 676–678.
- [3] Khaerudini, D.S., Guan, G., Zhang, P., Hao, X., and Abudula, A., 2014, Prospects of oxide ionic conductivity bismuth vanadate-based solid electrolytes, *Rev. Chem. Eng.*, 30 (6), 539–551.
- [4] Tripathy, D., Saikia, A., and Pandey, A.C., 2019, Effect of simultaneous Ti and Nb doping on structure and ionic conductivity of $\text{Bi}_2\text{V}_{1-x}\text{Ti}_{x/2}\text{Nb}_{x/2}\text{O}_{5.5-\delta}$ ($0.1 \leq x \leq 0.25$) ceramics, *Ionics*, 25 (5), 2221–2230.
- [5] Tripathy, D., and Pandey, A., 2018, Structural and impedance studies of Ti^{IV} and Nb^{V} co-doped bismuth vanadate system, *J. Alloys Compd.*, 737, 136–143.
- [6] Pernot, E., Anne, M., Bacmann, M., Strobel, P., Fouletier, J., Vannier, R.N., Mairesse, V.G., Abraham, F., and Nowogrocki, G., 1994, Structure and conductivity of Cu and Ni-substituted $\text{Bi}_4\text{V}_2\text{O}_{11}$ compounds, *Solid State Ionics*, 70-71, 259–263.
- [7] Abrahams, I., Krok, F., Malys, M., and Bush, A.J., 2001, Defect structure and ionic conductivity as a function of thermal history in BIMGVOX solid electrolytes, *J. Mater. Sci.*, 36 (5), 1099–1104.
- [8] Rusli, R., Abrahams, I., Patah, A., Prijamboedi, B., and Ismunandar, 2014, Ionic conductivity of $\text{Bi}_2\text{Ni}_x\text{V}_{1-x}\text{O}_{5.5-3x/2}$ ($0.1 \leq x \leq 0.2$) oxides prepared by a low temperature sol-gel route, *AIP Conf. Proc.*, 1589 (1), 178.
- [9] Abraham, F., Boivin, J.C., Mairesse, G., and Nowogrocki, G., 1990, The BIMEVOX series: A new family of high performances oxide ion conductors, *Solid State Ionics*, 40-41, 934–937.
- [10] Abrahams, I., and Krok, F., 2002, Defect chemistry of the BIMEVOXes, *J. Mater. Chem.*, 12 (12), 3351–3362.

- [11] Khaerudini, D.S., Guan, G., Zhang, P., Hao, X., Kasai, Y., Kusakabe, K., and Abudula, A., 2014, Structural and conductivity characteristics of $\text{Bi}_4\text{Mg}_x\text{V}_{2-x}\text{O}_{11-\delta}$ ($0 \leq x \leq 0.3$) as solid electrolyte for intermediate temperature SOFC application, *J. Alloys Compd.*, 589, 29–36.
- [12] Kant, R., Singh, K., and Pandey, O.P., 2010, Structural, thermal and transport properties of $\text{Bi}_4\text{V}_{2-x}\text{Ga}_x\text{O}_{11-\delta}$ ($0 \leq x \leq 0.4$), *Ionics*, 16 (3), 277–282.
- [13] Dereeper, E., Briois, P., and Billard, A., 2017, BITAVOX coatings obtained by reactive magnetron sputtering: Influence of thickness and composition, *Solid State Ionics*, 304, 7–12.
- [14] Kant, R., Singh, K., and Pandey, O.P., 2008, Synthesis and characterization of bismuth vanadate electrolyte material with aluminium doping for SOFC application, *Int. J. Hydrogen Energy*, 33 (1), 455–462.
- [15] Krok, F., Abrahams, I., Zadrožna, A., Małys, M., Bogusz, W., Nelstrop, J.A.G., and Bush, A.J., 1999, Electrical conductivity and structure correlation in BIZNVOX, *Solid State Ionics*, 119 (1-4), 139–144.
- [16] Mairesse, G., 1999, Advances in oxygen pumping concept with BIMEVOX, *C. R. Acad. Sci. IIC: Chim.*, 2 (11-13), 651–660.
- [17] Mairesse, G., Roussel, P., Vannier, R.N., Anne, M., Pirovano, C., and Nowogrocki, G.L., 2003, Crystal structure determination of α , β and γ - $\text{Bi}_4\text{V}_2\text{O}_{11}$ polymorphs. Part I: γ and β - $\text{Bi}_4\text{V}_2\text{O}_{11}$, *Solid State Sci.*, 5 (6), 851–859.
- [18] Payne M.C., and TCM group in Cambridge, 2005, *CASTEP of Material Studio Modeling from Accerys*, series number 3.2.00, with consumer is Politecnico di Torino.
- [19] Gale, J.D., 1997, GULP: A computer program for the symmetry-adapted simulation of solids, *J. Chem. Soc., Faraday Trans.*, 93 (4), 629–637.
- [20] Todorov, I.T., Smith, W., Trachenko, K., and Dove, M.T., 2006, DL_POLY_3: New dimensions in molecular dynamics simulations via massive parallelism, *J. Mater. Chem.*, 16 (20), 1911–1918.
- [21] Voronkova, V.I., Yanovskii, V.K., Kharitonova, E.P., and Rudnitskaya, O.G., 2005, Superionic conductors in the Bi_2WO_6 - $\text{Bi}_2\text{VO}_{5.5}$ system, *Inorg. Mater.*, 41 (7), 760–765.
- [22] Kant, R., Singh, K., and Pandey, O.P., 2009, Microstructural and electrical behavior of $\text{Bi}_4\text{V}_{2-x}\text{Cu}_x\text{O}_{11-\delta}$ ($0 \leq x \leq 0.4$), *Ceram. Int.*, 35 (1), 221–227.
- [23] Lazure, S., Vernochet, C., Vannier, R.N., Nowogrocki, G., and Mairesse, G., 1996, Composition dependence of oxide anion conduction in the BIMEVOX family, *Solid State Ionics*, 90 (1-4), 117–123.
- [24] Murasheva, V.V., Fortalnova, E.A., Politova, E.A., Politova, E.D., Safronenko, M.G., Stefanovich, S.Y., and Venskovskii, N.U., 2008, Phase transitions in the BIMEVOX solid solutions with $\text{Me} = \text{Ga}, \text{Zr}$, *Mater. Sci. Forum*, 587-588, 114–117.
- [25] Joubert, O., Jouanneaux, A., Ganne, M., Vannier, R.N., and Mairesse, G., 1994, Solid phase synthesis and characterization of new BIMEVOX series: $\text{Bi}_4\text{V}_{2-x}\text{M}_x\text{O}_{11}$ ($\text{M} = \text{Sb}^{\text{V}}, \text{Nb}^{\text{V}}$), *Solid State Ionics*, 73 (3-4), 309–318.
- [26] Ramsahye, N.A., and Bell, R.G., 2005, Cation mobility and the sorption of chloroform in zeolite NaY: Molecular dynamics study, *J. Phys. Chem. B*, 109 (10), 4738–4747.
- [27] Guillodo, M., Bassat, J.M., Fouletier, J., Dessemond, L., and Del Gallo, P., 2003, Oxygen diffusion coefficient and oxygen exchange coefficient of BIMEVOX.10 ($\text{ME} = \text{Cu}, \text{Co}$) ceramic membranes, *Solid State Ionics*, 164 (1-2), 87–96.
- [28] Krok, F., Bogusz, W., Kurek, P., Wasiucionek, M., Jakubowski, W., and Dygas, J., 1993, Influence of preparation procedure on some physical properties of BICUVOX, *Mater. Sci. Eng., B*, 21 (1), 70–76.
- [29] Simner, S.P., Suarez-Sandoval, D., Mackenzie, J.D., and Dunn, B., 1997, Synthesis, densification, and conductivity characteristics of BICUVOX oxygen-conducting ceramics, *J. Am. Ceram. Soc.*, 80 (10), 2563–2568.